Characteristics of paraxial propagation of a super Lorentz–Gauss SLG_{01} mode in uniaxial crystal orthogonal to the optical axis*

Zhou Guo-Quan(周国泉)†

School of Sciences, Zhejiang A & F University, Lin'an 311300, *China*

(Received 28 August 2011; revised manuscript received 20 September 2011)

Analytical propagation expression of a super Lorentz–Gauss $(SLG)_{01}$ mode in uniaxial crystal orthogonal to the optical axis is derived. The SLG_{01} mode propagating in uniaxial crystal orthogonal to the optical axis mainly depends on the ratio of the extraordinary refractive index to the ordinary refractive index. The SLG_{01} mode propagating in uniaxial crystals becomes an astigmatic beam. The beam spot of the SLG_{01} mode in the uniaxial crystal is elongated in the x- or y-direction, which is determined by the ratio of the extraordinary refractive index to the ordinary refractive index. With the increase of the deviation of the ratio of the extraordinary refractive index to the ordinary refractive index from unity, the elongation of the beam spot also augments. In different observation planes, the phase distribution of an SLG_{01} mode in the uniaxial crystal takes on different shapes. With the variation of the ratio of the extraordinary refractive index to the ordinary refractive index, the phase distribution is elongated in one transversal direction and is contracted in the other perpendicular direction. This research is beneficial to the practical applications of an SLG mode.

Keywords: super Lorentz–Gauss mode, uniaxial crystals, paraxial propagation

PACS: 41.85.Ew, 42.25.Bs, 42.60.Jf, 42.70.–a **DOI:** 10.1088/1674-1056/21/5/054104

1. Introduction

Due to its highly angular spreading, the Lorentz–Gauss beam has been introduced to describe the radiation emitted by a diode laser.[1,2] The properties of a Lorentz–Gauss beam have been widely investigated and well mastered.[3−10] However, the Lorentz–Gauss beam is only valid for the description of the fundamental mode emitted by a diode laser. Therefore, an orthogonal beam family of super Lorentz–Gauss (SLG) modes has been proposed to describe the high-order mode emitted by diode lasers.[11] The SLG_{00} mode is just the Lorentz–Gauss beam. As a classical representative of the high-order mode, the SLG_{01} mode is usually selected to be the research object. The properties of paraxial and non-paraxial propagations of the SLG_{01} mode have been examined in free space.[11,12] The vectorial structure of the SLG_{01} mode has been revealed in the far-field regime.[13] The characteristics of the average intensity and the effective beam size of the SLG_{01} mode in turbulent atmosphere have been evaluated.[14] Also, the SLG_{01} mode extends to the partially coherent case. The mutual coherence function and the spatial complex degree of coherence for the partially coherent SLG_{01} mode through a paraxial and real $ABCD$ optical system have been derived, and the corresponding physical pictures have been demonstrated.[15] The reported researches indicate that SLG modes are more appropriate than Hermite–Gaussian beams to describe the high-order modes emitted by diode lasers.

In addition to in free space and in turbulent atmosphere, laser beams also propagate in anisotropic medium such as uniaxial crystals, which is treated by solving Maxwell equations. Some applications, e.g. the design of the polarizer and the compensator, are involved in laser beams propagating in uniaxial crystals. The propagations of various kinds of laser beams in uniaxial crystals have been extensively investigated.[16−22] To the best of our knowledge, however, no literature dealing with the propagation of a high-order SLG mode in uniaxial crystal has been reported. In the remainder of this paper, therefore, the paraxial propagation of an SLG_{01} mode in uniaxial

*Project supported by the National Natural Science Foundation of China (Grant No. 10974179) and the Natural Science Foundation of Zhejiang Province, China (Grant No. Y1090073).

†Corresponding author. E-mail: zhouguoquan178@sohu.com

© 2012 Chinese Physical Society and IOP Publishing Ltd

crystal orthogonal to the optical axis is to be examined.

2. Paraxial propagation of an SLG_{01} mode in uniaxial crystal orthogonal to the optical axis

In the Cartesian coordinate system, the z-axis is taken to be the propagation axis. The optical axis of the uniaxial crystal coincides with the x-axis. The input plane is at $z = 0$ and the observation plane is at position z. The dielectric tensor of the uniaxial crystal is described by

$$\varepsilon = \begin{pmatrix} n_{\rm e}^2 & 0 & 0 \\ 0 & n_{\rm o}^2 & 0 \\ 0 & 0 & n_{\rm o}^2 \end{pmatrix}, \tag{1}$$

where $n_{\rm o}$ and $n_{\rm e}$ are the ordinary and the extraordinary refractive indices, respectively. The SLG_{01} mode considered here is linearly polarized in the x-direction and is incident on a uniaxial crystal in the plane $z = 0$. The SLG_{01} mode in the input plane $z = 0$ is given in the form of [11]

$$\begin{bmatrix} E_x(x_0, y_0, 0) \\ E_y(x_0, y_0, 0) \end{bmatrix} = \begin{bmatrix} \left(\dfrac{1}{w_0^2} + \dfrac{1}{w_{0y}^2}\right)^{1/2} \dfrac{w_{0x}^2}{w_{0x}^2 + x_0^2} \exp\left(-\dfrac{x_0^2}{w_0^2}\right) \dfrac{w_{0y}^2 y_0}{w_{0y}^2 + y_0^2} \exp\left(-\dfrac{y_0^2}{w_0^2}\right) \\ 0 \end{bmatrix}, \tag{2}$$

where w_0 is the waist of the Gaussian part; w_{0x} and w_{0y} are the width parameters of the Lorentzian part in the x- and y-directions, respectively. Within the framework of the paraxial approximation, the propagation of the SLG_{01} mode in uniaxial crystal orthogonal to the optical axis obeys the following equations:[23]

$$\begin{aligned} & E_x(x, y, z) \\ = & \frac{kn_{\rm o}}{2\pi {\rm i}z} \exp({\rm i}kn_{\rm e}z) \int_{-\infty}^{\infty}\int_{-\infty}^{\infty} E_x(x_0, y_0, 0) \\ & \times \exp\left\{ -\frac{k}{2{\rm i}zn_{\rm e}}[n_{\rm o}^2(x - x_0)^2 \right. \\ & \left. + n_{\rm e}^2(y - y_0)^2]\right\} {\rm d}x_0\,{\rm d}y_0, \end{aligned} \tag{3}$$

$$\begin{aligned} & E_y(x, y, z) \\ = & \frac{kn_{\rm o}}{2\pi {\rm i}z} \exp({\rm i}kn_{\rm o}z) \int_{-\infty}^{\infty}\int_{-\infty}^{\infty} E_y(x_0, y_0, 0) \\ & \times \exp\left\{ -\frac{kn_{\rm o}}{2{\rm i}z}\left[(x - x_0)^2 + (y - y_0)^2\right]\right\} {\rm d}x_0\,{\rm d}y_0, \end{aligned} \tag{4}$$

where $k = 2\pi/\lambda$ is the wave number with λ being the optical wavelength. Inserting Eq. (2) into Eq. (3), we can obtain

$$\begin{aligned} E_x(x, y, z) = & \frac{kn_{\rm o}}{2\pi iz}\left(\frac{1}{w_0^2} + \frac{1}{w_{0y}^2}\right)^{1/2} \\ & \times \exp({\rm i}kn_{\rm e}z) E_x(x, z) E_y(y, z), \end{aligned} \tag{5}$$

with $E_x(x, z)$ and $E_y(y, z)$ being given by

$$\begin{aligned} E_x(x, z) = & \int_{-\infty}^{\infty} \frac{w_{0x}^2}{w_{0x}^2 + x_0^2} \exp\left(-\frac{x_0^2}{w_0^2}\right) \\ & \times \exp\left[-\frac{kn_{\rm o}^2}{2{\rm i}zn_{\rm e}}(x - x_0)^2\right] {\rm d}x_0, \end{aligned} \tag{6}$$

$$\begin{aligned} E_y(y, z) = & \int_{-\infty}^{\infty} \frac{w_{0y}^2 y_0}{w_{0y}^2 + y_0^2} \exp\left(-\frac{y_0^2}{w_0^2}\right) \\ & \times \exp\left[-\frac{kn_{\rm e}}{2{\rm i}z}(y - y_0)^2\right] {\rm d}y_0. \end{aligned} \tag{7}$$

Equation (6) can be rewritten as

$$\begin{aligned} & E_x(x, z) \\ = & w_{0x}^2 \exp\left[\frac{kn_{\rm o}(1 - a)x^2}{2{\rm i}eaz}\right] \\ & \times \int_{-\infty}^{\infty} \frac{1}{w_{0x}^2 + x_0^2} \exp\left[-\frac{kn_{\rm o}a}{2{\rm i}ez}\left(\frac{x}{a} - x_0\right)^2\right] {\rm d}x_0, \end{aligned} \tag{8}$$

with the auxiliary parameters e and a being defined by

$$e = \frac{n_{\rm e}}{n_{\rm o}}, \quad a = 1 + \frac{2{\rm i}ez}{kn_{\rm o}w_0^2}. \tag{9}$$

We note that the convolution of two functions, $f_1(\tau)$ and $f_2(\tau)$, is defined by[24]

$$f_1(\tau) * f_2(\tau) = \int_{-\infty}^{\infty} f_1(x_0) f_2(\tau - x_0) {\rm d}x_0, \tag{10}$$

where the asterisk denotes the convolution. Therefore, Eq. (8) can be expressed in the form of the convolution as

$$\begin{aligned} E_x(x, z) = & w_{0x}^2 \exp\left[\frac{kn_{\rm o}(1 - a)x^2}{2{\rm i}eaz}\right] \\ & \times \left[f_1\left(\frac{x}{a}\right) * f_2\left(\frac{x}{a}\right)\right], \end{aligned} \tag{11}$$

where the auxiliary functions $f_1(\tau)$ and $f_2(\tau)$ are given by

$$f_1(\tau) = \frac{1}{w_{0x}^2 + \tau^2}, \tag{12}$$

$$f_2(\tau) = \exp\left(-\frac{kn_\mathrm{o}a}{2\mathrm{i}ez}\tau^2\right). \tag{13}$$

The convolution theorem of the Fourier transform has[24]

$$f_1(\tau) * f_2(\tau) = \int_{-\infty}^{\infty} f_1(\xi) f_2(\xi) \exp(-\mathrm{i}\xi\tau)\mathrm{d}\xi, \tag{14}$$

where the auxiliary functions $f_1(\xi)$ and $f_2(\xi)$ are the Fourier transforms of $f_1(\tau)$ and $f_2(\tau)$, respectively. $f_1(\xi)$ and $f_2(\xi)$ are given by

$$\begin{aligned} f_1(\xi) &= \frac{1}{\sqrt{2\pi}}\int_{-\infty}^{\infty} f_1(\tau)\exp(\mathrm{i}\xi\tau)\mathrm{d}\tau \\ &= \frac{1}{\sqrt{2\pi}}\int_{-\infty}^{\infty} \frac{1}{w_{0x}^2+\tau^2}\exp(\mathrm{i}\xi\tau)\mathrm{d}\tau \\ &= \sqrt{\frac{\pi}{2w_{0x}^2}}\exp(-w_{0x}|\xi|), \end{aligned} \tag{15}$$

$$\begin{aligned} f_2(\xi) &= \frac{1}{\sqrt{2\pi}}\int_{-\infty}^{\infty} f_2(\tau)\exp(\mathrm{i}\xi\tau)\mathrm{d}\tau \\ &= \frac{1}{\sqrt{2\pi}}\int_{-\infty}^{\infty} \exp\left(-\frac{kn_\mathrm{o}a}{2\mathrm{i}ez}\tau^2\right)\exp(\mathrm{i}\xi\tau)\mathrm{d}\tau \\ &= \sqrt{\frac{\mathrm{i}ez}{kn_\mathrm{o}a}}\exp\left(-\frac{\mathrm{i}ez}{2kn_\mathrm{o}a}\xi^2\right). \end{aligned} \tag{16}$$

Therefore, equation (11) turns into

$$\begin{aligned} E_x(x,z) &= w_{0x}\sqrt{\frac{\mathrm{i}\pi ez}{2kn_\mathrm{o}a}}\exp\left[\frac{kn_\mathrm{o}(1-a)x^2}{2\mathrm{i}eaz}\right]\int_{-\infty}^{\infty}\exp(-w_{0x}|\xi|)\exp\left(-\frac{\mathrm{i}ez}{2kn_\mathrm{o}a}\xi^2\right)\exp\left(-\frac{\mathrm{i}x}{a}\xi\right)\mathrm{d}\xi \\ &= w_{0x}\sqrt{\frac{\mathrm{i}\pi ez}{2kn_\mathrm{o}a}}\exp\left[\frac{kn_\mathrm{o}(1-a)x^2}{2\mathrm{i}eaz}\right]\left\{\int_0^{\infty}\exp\left\{-\frac{\mathrm{i}ez}{2kn_\mathrm{o}a}\left[\xi+\frac{kn_\mathrm{o}a}{\mathrm{i}ez}\left(w_{0x}+\mathrm{i}\frac{x}{a}\right)\right]^2\right\}\mathrm{d}\xi\right. \\ &\quad\times\exp\left[\frac{kn_\mathrm{o}a}{2\mathrm{i}ez}\left(w_{0x}+\mathrm{i}\frac{x}{a}\right)^2\right] + \int_0^{\infty}\exp\left\{-\frac{\mathrm{i}ez}{2kn_\mathrm{o}^a}\left[\xi+\frac{kn_\mathrm{o}a}{\mathrm{i}ez}\left(w_{0x}-\mathrm{i}\frac{x}{a}\right)\right]^2\right\}\mathrm{d}\xi \\ &\quad\left.\times\exp\left[\frac{kn_\mathrm{o}a}{2\mathrm{i}ez}\left(w_{0x}-\mathrm{i}\frac{x}{a}\right)^2\right]\right\}. \end{aligned} \tag{17}$$

After performing the integral, we have

$$\begin{aligned} E_x(x,z) &= \frac{\pi w_{0x}}{2}\exp\left[\frac{kn_\mathrm{o}(1-a)x^2}{2\mathrm{i}eaz}\right] \\ &\quad\times[U_x^+(x,z)+U_x^-(x,z)], \end{aligned} \tag{18}$$

with $U_x^{\pm}(x,z)$ being given by

$$\begin{aligned} U_x^{\pm}(x,z) &= \exp\left[\frac{kn_\mathrm{o}a}{2\mathrm{i}ez}\left(w_{0x}\pm\mathrm{i}\frac{x}{a}\right)^2\right] \\ &\quad\times\mathrm{erfc}\left[\sqrt{\frac{kn_\mathrm{o}a}{2\mathrm{i}ez}}\left(w_{0x}\pm\mathrm{i}\frac{x}{a}\right)\right], \end{aligned} \tag{19}$$

where $\mathrm{erfc}(\cdot)$ is the complementary error function. Similarly, Eq. (7) is found to be

$$\begin{aligned} E_y(y,z) &= \frac{\mathrm{i}\pi w_{0y}^2}{2}\exp\left[\frac{ken_\mathrm{o}(1-b)y^2}{2\mathrm{i}bz}\right] \\ &\quad\times[V_y^+(y,z)-V_y^-(y,z)], \end{aligned} \tag{20}$$

with b and $V_y^{\pm}(y,z)$ being given by

$$b = 1+\frac{2\mathrm{i}z}{ken_\mathrm{o}w_0^2}, \tag{21}$$

$$\begin{aligned} V_y^{\pm}(y,z) &= \exp\left[\frac{ken_\mathrm{o}b}{2\mathrm{i}z}\left(w_{0y}\pm\mathrm{i}\frac{y}{b}\right)^2\right] \\ &\quad\times\mathrm{erfc}\left[\sqrt{\frac{ken_\mathrm{o}b}{2\mathrm{i}z}}\left(w_{0y}\pm\mathrm{i}\frac{y}{b}\right)\right]. \end{aligned} \tag{22}$$

As a result, the analytical paraxial propagation equations of an SLG_{01} mode in uniaxial crystals orthogonal to the optical axis yield

$$\begin{aligned} &E_x(x,y,z) \\ &= \frac{\pi kn_\mathrm{o}w_{0x}w_{0y}^2}{8z}\left(\frac{1}{w_0^2}+\frac{1}{w_{0y}^2}\right)^{1/2}\exp(\mathrm{i}ken_\mathrm{o}z) \\ &\quad\times\exp\left[\frac{kn_\mathrm{o}}{2\mathrm{i}z}\left(\frac{1-a}{ae}x^2+\frac{1-b}{b}ey^2\right)\right] \\ &\quad\times[U_x^+(x,z)+U_x^-(x,z)][V_y^+(y,z)-V_y^-(y,z)], \end{aligned} \tag{23}$$

$$E_y(x,y,z) = 0. \tag{24}$$

3. Numerical results and analyses

According to the analytical formulae derived in the last section, here we investigate the propagation properties of an SLG_{01} mode in the uniaxial crystal orthogonal to the optical axis. Here we pay attention mainly to the influence of the uniaxial crystal on

the propagation of an SLG_{01} mode. Calculation parameters are chosen to be $\lambda = 0.8$ μm, $n_o = 2.616$, $w_0 = 2$ mm, $w_{0x} = 1.5$ mm, and $w_{0y} = 1.5$ mm. The top row of Fig. 1 represents the contour graph of the normalized intensity of a SLG_{01} mode propagating in the uniaxial crystal orthogonal to the optical axis in several observation planes where $e = 1.5$. For convenience, the normalized intensity of an SLG_{01} mode propagating in free space is also plotted in the bottom row of Fig. 1. The three observation planes are at $z = 0.1z_r$, $z = 0.5z_r$, and $z = z_r$, where $z_r = kw_0^2/2$ is the Rayleigh length of the Gaussian part. Upon propagation in the uniaxial crystal orthogonal to the optical axis, the spreading of the SLG_{01} mode in the y-direction is far slower than in the x-direction, which is caused by the anisotropic effect of the crystal. As a result, the beam spot of the SLG_{01} mode propagating in the uniaxial crystals is elongated in the x-direction. Upon propagation in free space, the spreading of the SLG_{01} mode is uniform in all directions. Secondly, the spreading of the SLG_{01} mode in the uniaxial crystal is far slower than in free space. Figure 2 shows the contours of the normalized intensity of an SLG_{01} mode propagating in the uniaxial crystals with $e = 2$. With increasing e value, the elongation of the beam spot in the x-direction of SLG_{01} mode propagating in the uniaxial crystal also augments, which can be obtained by comparing Fig. 2 with Fig. 1. The value of e in Figs. 1 and 2 is larger than unity. Of course, sometimes the e value is likely to be smaller than unity, which is demonstrated in Figs. 3 and 4. The values of e are 0.9 and 0.6 in Figs. 3 and 4 respectively. When $e < 1$, the beam spot of the SLG_{01} mode propagating in the uniaxial crystal is elongated in the y-direction. With decreasing e value, moreover, the elongation of the beam spot in the y-direction of SLG_{01} mode propagating in the uniaxial crystal increases.

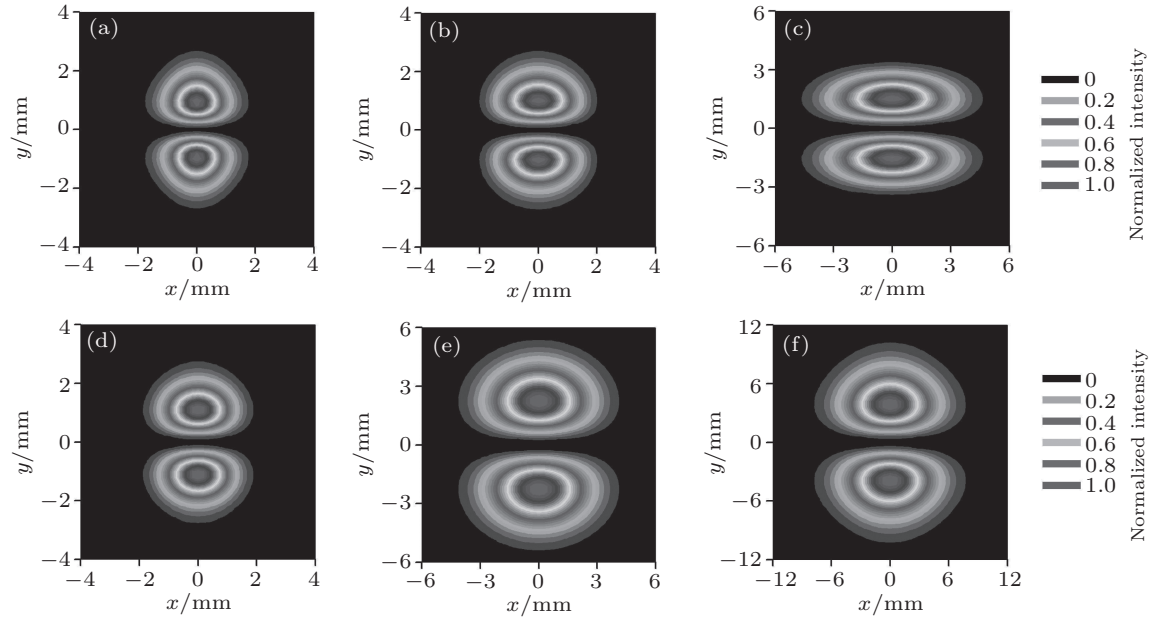


Fig. 1. Contours of the normalized intensity of an SLG_{01} mode propagating in the uniaxial crystal (the top row) and in free space (the bottom row) in several observation planes at $z = 0.1z_r$ ((a) and (d)), $0.5z_r$ ((b) and (e)), and z_r ((c) and (f)), with $e = 1.5$.

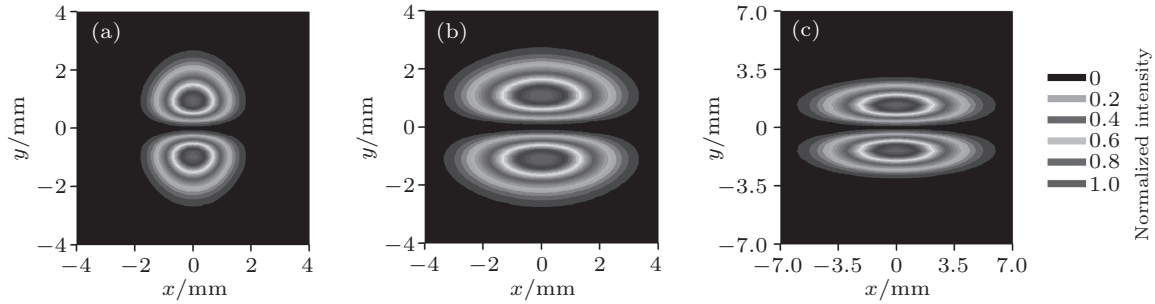


Fig. 2. Contours of the normalized intensity of an SLG_{01} mode propagating in the uniaxial crystals in several observation planes at $z = 0.1z_r$ (a), $0.5z_r$ (b), and z_r (c), with $e = 2$.

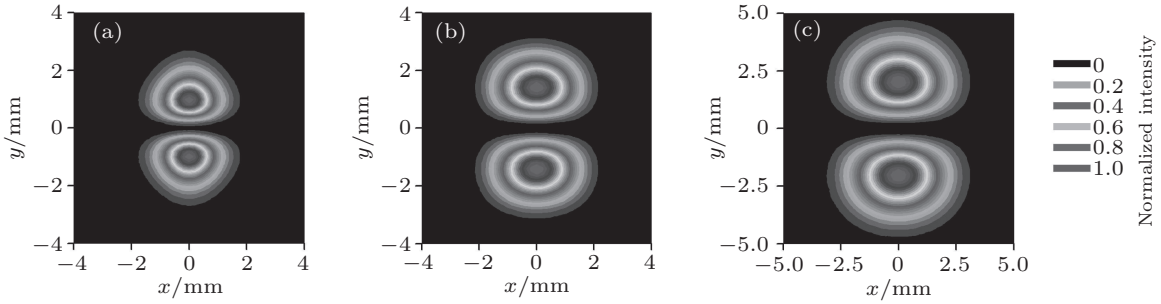


Fig. 3. Contours of the normalized intensity of an SLG_{01} mode propagating in the uniaxial crystals in several observation planes at $z = 0.1z_r$ (a), $0.5z_r$ (b), and z_r (c), with $e = 0.9$.

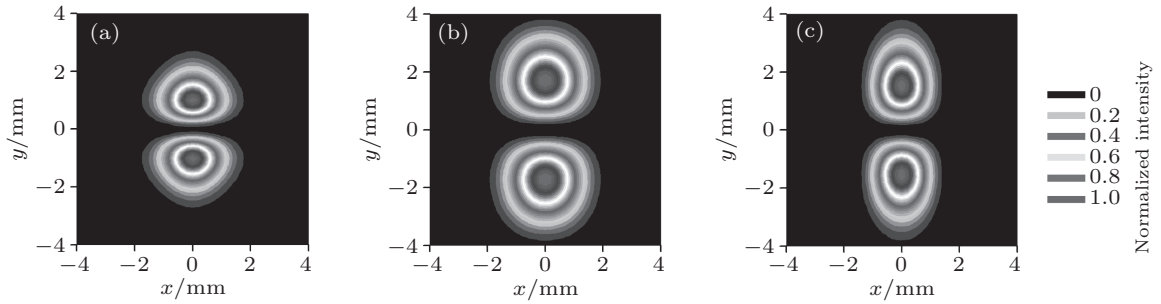


Fig. 4. Contours of the normalized intensity of an SLG_{01} mode propagating in the uniaxial crystals in several observation planes at $z = 0.1z_r$ (a), $0.5z_r$ (b), and z_r (c), with $e = 0.6$.

Figures 5–7 represent the contours of the phase of an SLG_{01} mode propagating in the uniaxial crystals with $e = 1.5$, 0.9, and 0.6, respectively. Figures 5–7 correspond to $z = 0.1z_r$, $z = 0.5z_r$, and $z = z_r$, respectively. The scales of the y-axis in Figs. 5(b) and 5(c) are the same as that in Fig. 5(a), so they are not marked to save space. In the observation plane $z = 0.1z_r$, the phase distribution of an SLG_{01} mode propagating in the uniaxial crystal is of diamond phase. Moreover, the phase in the central region is minimum. With increasing e value, the magnitude of the phase increases and the phase in the x-axis of the central region also dramatically increases. With decreasing e value, the diamond phase distribution is elongated in the x-direction and is contracted in the y-direction. In the observation plane at $z = 0.5z_r$, the phase distribution of an SLG_{01} mode propagating in the uniaxial crystal takes on trumpet shape. With decreasing e value, the phase in the central region also decreases. Moreover, the trumpet-shaped phase distribution is elongated in the x-direction and is contracted in the y-direction. In the observation plane at $z = z_r$, the phase distribution is gear shaped. With decreasing e value, the gear shaped phase distribution is elongated in the y-direction and is contracted in the x-direction. The phase in the central region besides the x-axis is maximum. With the value of e decreasing, the central maximum region augments.

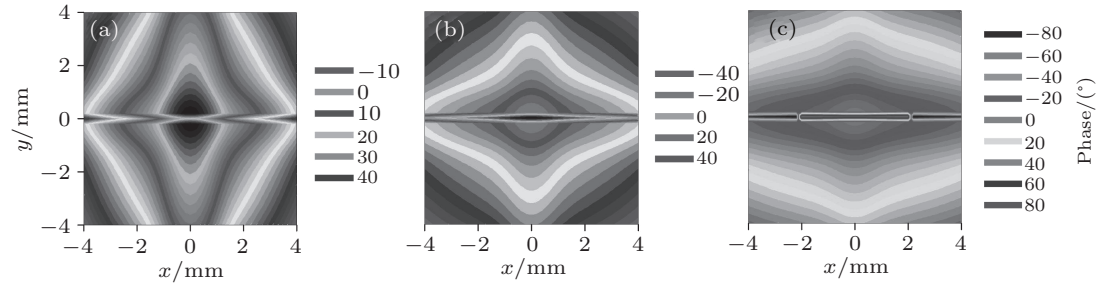


Fig. 5. Contours of the phase of an SLG_{01} mode propagating in the uniaxial crystals in the observation plane at $z = 0.1z_r$, with $e = 1.5$ (a), 0.9 (b), and 0.6(c).

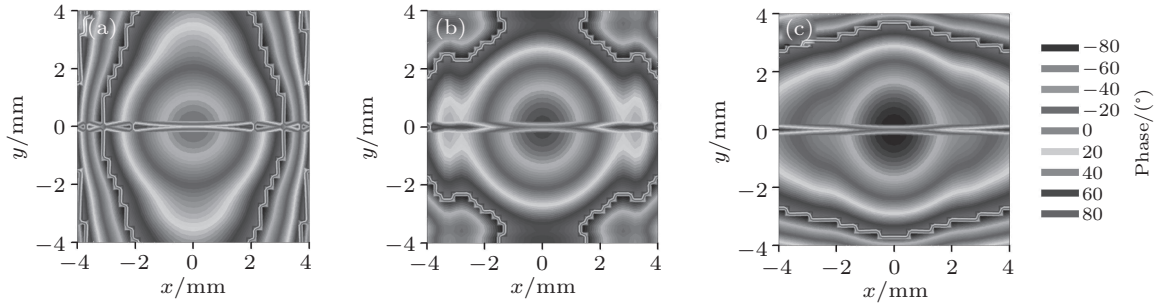


Fig. 6. Contours of the phase of an SLG_{01} mode propagating in the uniaxial crystals in the observation plane at $z = 0.5z_r$, with $e = 1.5$ (a), 0.9 (b), and 0.6 (c).

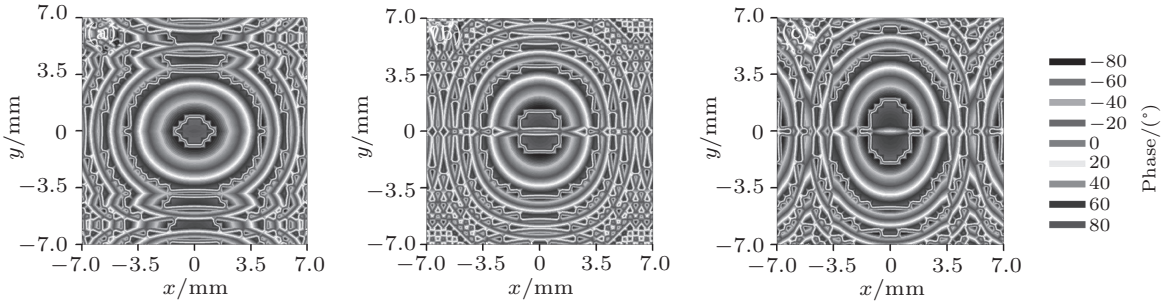


Fig. 7. Contours of the phase of an SLG_{01} mode propagating in the uniaxial crystals in the observation plane at $z = 1z_r$ with $e = 1.5$, 0.9 (b), and 0.6 (c).

4. Conclusions

An analytical propagation expression of the SLG_{01} mode in uniaxial crystal orthogonal to the optical axis is derived. The SLG_{01} mode propagating in uniaxial crystal orthogonal to the optical axis depends on ordinary refractive index n_o, the ratio of the extraordinary refractive index to the ordinary refractive index e, axial propagation distance z, and three beam parameters w_0, w_{0x}, and w_{0y}. The influence of the uniaxial crystal on the normalized intensity distribution of an SLG_{01} mode is numerically investigated. When $e > 1$, the beam spot of the SLG_{01} mode in the uniaxial crystal is elongated in the x-direction. With increasing e value, moreover, the elongation of the beam spot in the x-direction of the SLG_{01} mode in the uniaxial crystal also augments. When $e < 1$, the beam spot of the SLG_{01} mode in the uniaxial crystal is elongated in the y-direction. Moreover, the elongation of the beam spot in the y-direction of SLG_{01} mode in the uniaxial crystal increases with decreasing e value. No matter what the value of e is, the spreading of the SLG_{01} mode in the uniaxial crystal is far slower than that in free space. The effect of the uniaxial crystal on the phase distribution of an SLG_{01} mode in the uniaxial crystal is also examined. In the different observation planes, the phase distribution of an SLG_{01} mode in the uniaxial crystal takes on different shapes. With decreasing e value, the phase distribution of an SLG_{01} mode in the observation plane at $z = 0.1z_r$ or $z = 0.5z_r$ is elongated in the x-direction and is contracted in the y-direction. In the observation plane at $z = z_r$, however, the phase distribution is elongated in the y-direction and is contracted in the x-direction with decreasing e value. The paraxial propagation of other more complicated SLG modes in uniaxial crystal orthogonal to the optical axis can be investigated by following the same procedure as that shown here. This research is beneficial to the practical applications of an SLG mode such as optical communications using uniaxial crystals.

References

[1] Naqwi A and Durst F 1990 *Appl. Opt.* **29** 1780
[2] Yang J, Chen T T, Ding G L and Yuan X 2008 *Proc. SPIE* **6824** 68240A
[3] Gawhary O E and Severini S 2006 *J. Opt.* A: *Pure Appl. Opt.* **8** 409
[4] Gawhary O E and Severini S 2007 *Opt. Commun.* **269** 274
[5] Torre A, Evans W A B, Gawhary O E and Severini S 2008 *J. Opt.* A: *Pure Appl. Opt.* **10** 115007
[6] Zhou G Q 2009 *Chin. Phys.* B **18** 2779
[7] Zhou P, Wang X L, Ma Y X, Ma H T, Xu X J and Liu Z J 2010 *J. Opt.* **12** 015409

[8] Zhou P, Wang X L, Ma Y X and Liu Z J 2010 *Appl. Opt.* **49** 2497
[9] Yu H, Xiong L L, Lü B D 2010 *Optik* **121** 1455
[10] Jiang Y F, Huang K K and Lu X H 2011 *Opt. Express* **19** 9708
[11] Zhou G Q 2010 *J. Opt. Soc. Am.* A **27** 563
[12] Zhou G Q 2010 *Chin. Phys.* B **19** 064201
[13] Zhou G Q 2010 *J. Opt.* **12** 035704
[14] Zhou G Q 2010 *Appl. Phys.* B **101** 371
[15] Zhou G Q 2010 *J. Opt.* **12** 055701
[16] Cincotti G, Ciattoni A and Palma C 2002 *J. Opt. Soc. Am.* A **19** 1680
[17] Lü B D and Luo S R 2004 *Opt. Laser. Technol.* **36** 51
[18] Liu D J and Zhou Z X 2008 *J. Opt.* A: *Pure Appl. Opt.* **10** 095005
[19] Deng D G, Yu H, Xu S Q, Shao J D and Fan Z X 2008 *Opt. Commun.* **281** 202
[20] Liu D J and Zhou Z X 2009 *J. Opt. Soc. Am.* A **26** 924
[21] Zhao C L and Cai Y J 2010 *J. Mod. Opt.* **57** 375
[22] Li J, Chen Y R, Xu S X, Wang Y Q, Zhou M C, Zhao Q, Xin Y and Chen F N 2011 *Opt. Laser Technol.* **43** 506
[23] Ciattoni A and Palma C 2003 *J. Opt. Soc. Am.* A **20** 2163
[24] Gradshteyn I and Ryzhik I 1980 *Table of Integrals, Series, and Products* (New York: Academic press)